Automatic Diagnosis of Melanoma: a Software System based on the 7-Point Check-List

G. Di Leo, A. Paolillo, P. Sommella
D.I.I.I.E. – University of Salerno (Italy)
{gdileo,apaolillo,psommella}@unisa.it

G. Fabbrocini
Dept of Dermatology – University of Naples "Federico II"
gfabbro@unina.it

Abstract

Early detection of melanoma is one of the greatest challenges of dermatologic practice today. A new diagnostic method, the "ELM 7 point checklist", defines a set of seven features, based on colour and texture parameters, which describe the malignancy of a lesion. It has been presented as faster and with the same accuracy than the traditional ABCD criteria in the diagnosis of melanoma. In this paper a new system for automated diagnosis of melanocytic skin lesions, based on ELM 7 point checklist, is introduced.

1. Introduction

Malignant melanoma is nowadays one of the leading cancer causes among many white-skinned populations. Indeed the earlier the diagnosis the lower the metastatic risk. The aim of prevention campaigns is to improve the early diagnosis of melanoma through the identification of precursors. The curability of skin cancer is nearly 100%, if it is recognized early enough and treated surgically.

Epiluminescence microscopy (ELM) is an in vivo, non invasive technique (see Figure 1) that has disclosed a new dimension of the clinical morphologic features of pigmented skin lesions, using different incident light magnification systems with an oil immersion technique ([1],[2]). Results of previous studies demonstrated that ELM improves accuracy in diagnosing pigmented skin lesions. Literature showed that dermoscopy had 10% to 27% higher sensitivity than clinical diagnosis by the naked eye.

Three diagnostic models with similar reliability have become more widely accepted by clinicians:

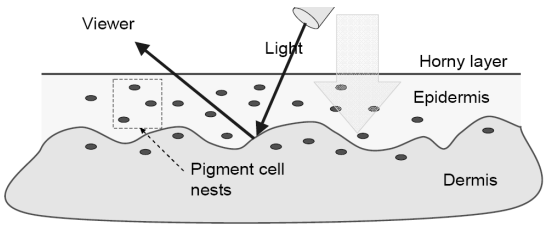

Figure 1. Epiluminescence dermoscopy

(i) pattern analysis, which is based on the "expert" qualitative assessment of numerous individual ELM criteria;

(ii) the ABCD-rule of dermatoscopy which is based on a semi-quantitative analysis of the following criteria: asymmetry (A), border (B), color (C) and different dermatoscopic (D) structures;

(iii) the ELM 7-point checklist scoring diagnosis analysis, proposed in [3] and defining only seven standard ELM criteria.

In order to calculate the ABCD score, the 'asymmetry, border, color, and differential structure' criteria have to be assessed semi-quantitatively [4]. Then, each of the criteria has to be multiplied by a given weight factor yielding a total dermoscopy score (TDS). TDS values less than 4.75 indicate a benign melanocytic lesion; values between 4.8 and 5.45 indicate a suspicious lesion and values greater than 5.45 are highly suspicious for melanoma.

The ELM 7-point checklist provides a simplification of standard pattern analysis and, if compared to ABCD, allows less experienced observers to achieve higher diagnostic accuracy values. The dermoscopic image of a melanocytic skin lesion is analyzed in order to detect the presence of these standard criteria; from this analysis a score is calculated. If a total score of 3 or more is assigned, the lesion is classified as melanoma; otherwise, it is classified as benign lesion.

Despite the simplification of the ELM criteria, all the diagnostic methods described showed higher reliability if they are based on a quantitative automated system. Consequently, the early diagnosis of skin cancer using digital image-processing methods, based on a semiquantitative scale, is a very important issue. Computerized identification could reduce the false positive or false negative clinical diagnosis because it adds a quantitative observation to the "clinical eye observation". In [5] Hoffmann reported that the combination of clinician and computer may potentially increase the accuracy of PSL (Pigmented Skin lesion)

IEEE computer society

978-0-7695-3869-3/10 $26.00

diagnosis. This may result in improved detection of melanoma and a reduction in unnecessary excision.

A growing interest has developed in the last decade in the automated analysis of digitized images obtained by epiluminescence microscopy techniques to assist clinicians in differentiating early melanoma from benign skin lesions [6].

Some automated systems, based on ABCD algorithm, have been developed. Ganster et al. [7] developed an automated melanoma recognition system but only 21 parameters were extracted from images. Schmid [8]-[9] proposed a color based segmentation scheme without extracting features. In [1] an automatic color segmentation algorithm with application to skin tumor feature identification was developed, whereas a new procedure based on the Catmull-Rom spline method and the computation of the gray-level gradient of points extracted by interpolation of normal direction on spline points was employed in [10].

Nevertheless, so far, no automated systems have yet been based on the 7-point checklist. From these considerations, and from previous experiences in digital processing of medical images ([11]), the authors have tackled the problem of defining suitable image processing algorithm implementing the 7-point checklist ([12]-[13]). It would be suitable to develop an automatic system that can validate the identification of 7 parameters on each lesion observed by clinicians.

This paper focuses on the main image processing techniques which can be suitably adopted for the development of a software tool which implements the 7-Point Check-List. Thus, the paper is organized as follows: the diagnostic method of interest is detailed in Section 2 with reference to the definition of the seven criteria. The architecture of the automatic diagnostic system is presented in Section 3, whereas Section 4 is devoted to the explanation of the images processing techniques adopted. Experimental results are presented in Section 5, and finally some conclusions are drawn in Section 6.

Table 1. the 7-point Check List score system

ELM criterion	Score
Major criteria	
1. Atypical pigment network	2
2. Blue-whitish veil	2
3. Atypical vascular pattern	2
Minor criteria	
4. Irregular streaks	1
5. Irregular pigmentation	1
6. Irregular dots/globules	1
7. Regression structures	1

2. The 7-Point Check List

The seven features concerning the dermoscopic criteria refer both to the chromatic characteristics and to the shape and/or texture of the lesion:

1) *Atypical Pigment Network*, black, brown, or gray network with irregular meshes and thick lines;
2) *Blue-whitish Veil*, confluent, gray-blue to whitish blue diffuse pigmentation associated with pigment network alteration, dots/globules and/or streaks;
3) *Atypical Vascular Pattern*, linear-irregular or dotted vessels not clearly combined with regression structures and associated with pigment network alterations, dots/globules and/or streaks;
4) *Irregular Streaks*, irregular, more or less confluent, linear structures not clearly combined with pigment network lines;
5) *Irregular Pigmentation*, black, brown and/or gray pigmented areas with irregular shape and/or distribution;
6) *Irregular Dots/Globules*, black, brown, and/or gray round to oval, variously sized structures irregularly distributed within the lesion;
7) *Regression Structures*, white scarlike depigmentation or peppering irregularly distributed within the lesion.

The definitions of the ELM criteria are briefly described in Table 1 along with the corresponding histological correlates.

As for the individual score (Table 2), there are three "major" criteria with an individual score equal to 2 and four "minor" criteria with an individual score equal to 1.

By a simple addition of the individual scores, the total score is obtained. Consequently in order to diagnose a melanoma, the identification of at least 2 melanoma-specific dermoscopic criteria (1 major plus 1 minor or 3 minor criteria) is required. Figure 2 shows two diagnosis examples where different structures are present and scores corresponding to melanomas are computed.

Thanks to the low number of features to identify and its scoring diagnostic system, the 7-point Check List can be easily learned and applied. Although experience can play an important role (different behavior can be attended by the ELM experts versus the non-experts) the method has proven to be reliable for diagnosing melanoma and if compared with the ABCD rule, allows better diagnostic accuracy values because of the tendency of the latter to over-classify atypical melanocytic nevi as melanomas.

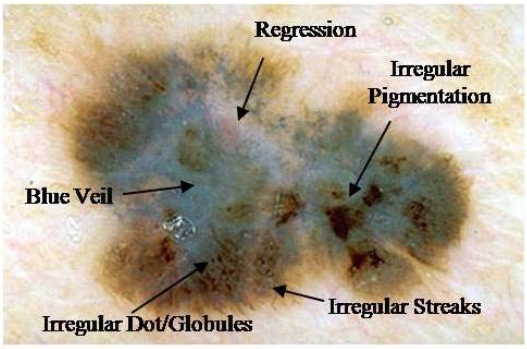

Figure 2. ELM image of a melanocytic lesion with several dermatoscopic criteria

3. The Automatic System

The automatic tool proposed for the diagnosis of skin lesions is based on the architecture suggested in [9]. The corresponding scheme is reported in Figure 3 suitably revisited. The input of the Computer aided System are digital images obtained by ELM which are processed through different algorithms derived from he clinical knowledge gained by expert dermatologists (well-trained in the 7-Point Check List application). In more details, the image processing relies on the detection of the lesion, which can be obtained with a boundary detection. Once the lesion is localized, different chromatic and morphological features can be quantified and used for classification. In order to train a classifier, images of benign and malignant lesions must be collected and stored in a database whereas the corresponding histopathology is adopted to set-up the diagnostic application. The collection of digital images can also serve as a reference database, where cases with known pathologies can be consulted by non expert dermatologists.

Besides supporting the physicians during the diagnosis phase, the software system is thought to also manage different computing resources. It provides an interface between the dermatologist and the image processing routines, allowing the storage and retrieval of unclassified and diagnosed cases, the access to the network and to a database server, the control of the digitization process (camera connected to the PC).

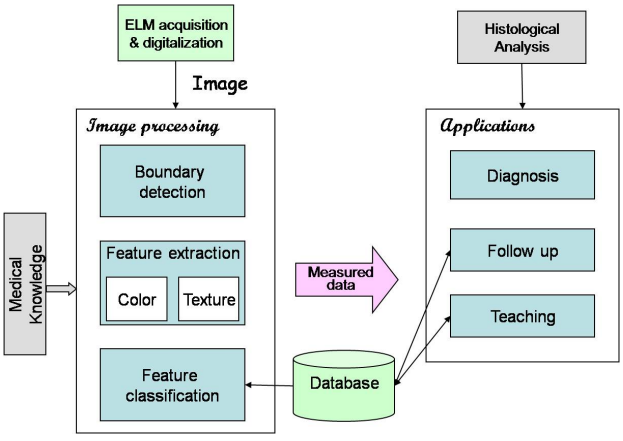

Figure 3. Scheme of the software tool for the diagnosis of pigmented lesion

4. The proposed methods

As reported in the scheme of Figure 3, the digital image processing is constituted by three main stages: the *boundary detection*, which allows the pigmented lesion to be extracted from the surrounding healthy skin, the *feature extraction* , which aims to measure morphological and chromatic features related to the dermoscopic structures of interest, and the *feature classification*, through which the detection of each criteria introduced in the 7_Point Check List is achieved. In the following, the methods and techniques adopted to perform the three stages are detailed.

4.1. Boundary detection

In general segmentation is the process of grouping pixels of a given image into regions homogenous with respect to certain features and to semantic content. The aim of the image segmentation stage is to extract the lesion border from the healthy skin. Boundary detection is a critical problem in dermatoscopic images because the transition between the lesion and the surrounding skin is smooth and hard to detect accurately, even for a trained dermatologist.

The realized segmentation algorithm for the skin lesion border extraction consists of three steps: (i) colour to monochrome image conversion; (ii) image binarization using an adaptive threshold; (iii) border identification.

(i) In the first step of the segmentation algorithm 3 different monochrome images (8 bits per pixel) are obtained from the source image (RGB standard color, 24 bits per pixel) corresponding to the red, green and blue color components, respectively (an example is reported in Figure 4). For each component, two modes are typically evident in the pixel intensity histogram corresponding respectively to the pigmented lesion and the surrounding skin.

(ii) The binarization (i.e. a conversion to a 1-bit/pixel format) of each monochrome image is carried out by thresholding the corresponding intensity histogram through a suitable value. Then, the image pixels with gray level lower than the threshold become black whilst the pixels greater than the threshold are set to white. More in detail, instead of choosing a fixed

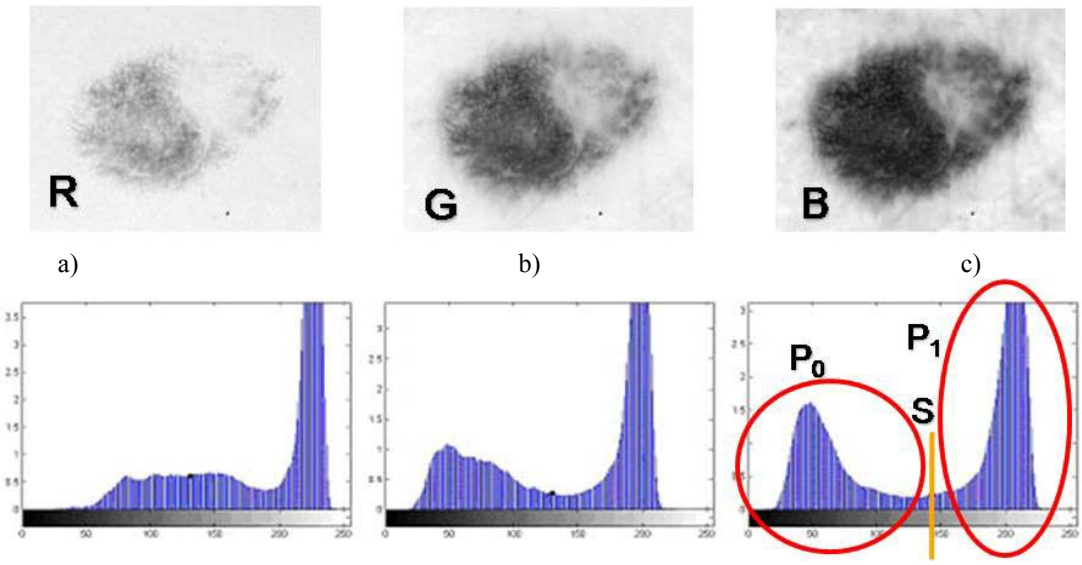

Figure 4. Monochrome images for Red, Green and Blue Planes and corresponding Intensity Histograms

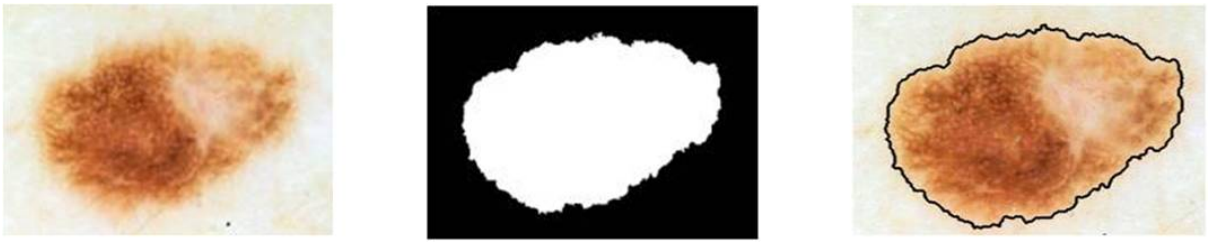

Figure 5. Results for the Boundary detection procedure
a) starting RGB image b) binary mask c) RGB image and superimposed contour

threshold at this point, an adaptive threshold is obtained for each monochrome image by adopting the Otsu algorithm [14]. Since this method aims to detect the thresholds (S) which maximize between-class variance and minimize the intra-class variance, the application of Otsu algorithm to a bimodal histogram usually provides very accurate results in the detection of the image background and foreground (corresponding to the histogram classes). Instead, the application of Otsu method to ELM images has been experimentally revealed to be more sensitive to surrounding skin (the image background). Consequently the thresholding result corresponding to the wider skin lesion area (the image foreground) has to be considered as binary mask for next processing. In the example of Figure 5.b the lesion appears in white against a black background, except for possible isolated black points in the white skin region. Hence, a morphological closing operator fills isolated black points in the white regions.

(iii) Finally, in order to extract the contour of the lesion, a simple blob-finding algorithm [9] is adopted for the binary image previously obtained: the tracking algorithm collects and sorts out the edges of the black-white image into an ordered list. At this point, the border is superimposed on the color ELM image (Figure 5.c) and displayed for visible inspection to the diagnostician. The binary image is also used in calculating the lesion dimension (number of white N_{tot}) that will be used in the lesion analysis.

4.2. Feature extraction

Because all the criteria of interest are related to single or particular combinations of both chromatic and morphological features, the extraction of the measured parameters of interest for next analysis can be performed adopting the two strategies:

- the *color segmentation*, with the aims to gain some basic information about color features (fundamental in detection of Blue Veil, Irregular Pigmentation, Regression and Vascular Pattern)
- the *texture extraction*, that aims to highlight basic morphological features (which mainly characterize the Atypical Pigment Network, Dot/globules, Irregular Streaks and newly Vascular Pattern).

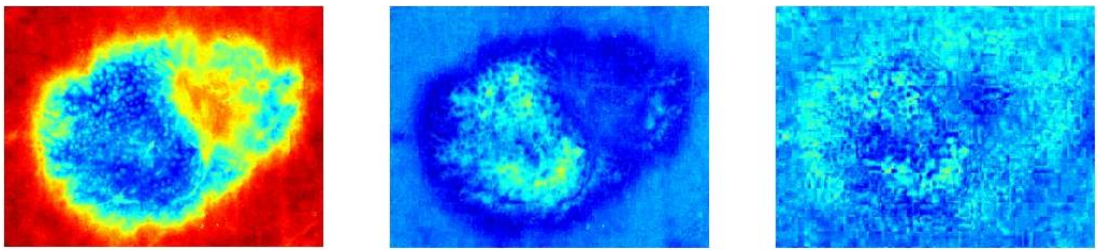

a) b) c)

Figure 6. Example of Hotelling Transformation:
a) 1st order Principal Component b) 2nd order Principal Component c) 3rd order Principal Component

4.2.1. Color segmentation. Starting from the source image and the binary mask, the lesion segmentation stage is carried out with the aim of splitting the internal area into multiple chromatically homogenous regions (the lesion map). The basic idea is the adoption of a suitable multithresholding of the colour image. In particular the following steps are proposed: (i) Principal Component Analysis (PCA); (ii) 2D histogram construction; (iii) peaks picking algorithm; (iv) histogram partitioning; (v) lesion partitioning.

(i) The Principal Component Analysis (also known as the discrete Karhunen-Loeve Transform or Hotelling Transform [15]) is a technique for reducing the dataset dimensionality while retaining those characteristics that contribute most to dataset variance. As for the application of the Principal Component Analysis to the ELM image, the RGB components of the pixels corresponding to lesion area (selected trough the binary mask obtained as final result of image segmentation) constitute the starting dataset (belonging to a state space with dimension N=3). A new 3D representation of the lesion pixels can be obtained from the Hotelling Transform equation. An example is reported in Figure 6: (for more evidence, PCA is related to all image pixels taking into account also the surrounding skin). The decreasing variability in each individual band as long as the order of the principal component increases can be noted easily.

(ii) Since the low order components preserve sufficient information in order to obtain reliable information (Figure 6.a-b) whereas the third component contains most of the image noise (Figure 6.c), the two principal components are used to compute a two-dimensional (2-D) histogram (referring to which the multithresholding has to be carried out). An example of 2-D histogram is depicted in Figure 7.a. Because the estimated histograms are, in general, noisy due to the scarcity of data, it is advantageous to smooth and down-sample the histograms to eliminate noise effects. In particular the original histogram is reduced from size 256x256 to size 64x64 (see Figure 7.b).

(iii) The multithresholding is carried out by finding peaks in the 2-D histogram with significant mass around them. It is expected that these peaks will

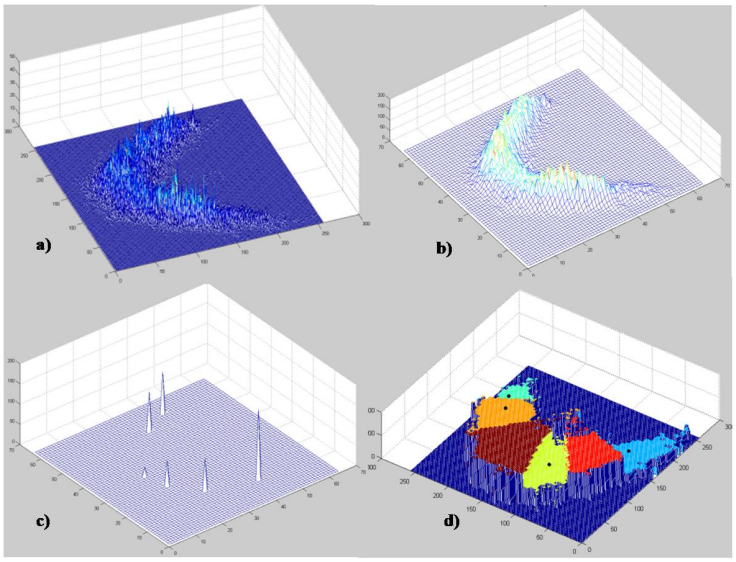

Figure 7. Construction and partitioning of 2-D histogram:
a) 2-D histogram; b) down-sampled 2-D histogram;
c) result of peak-picking method; d) partitioned 2-D histogram.

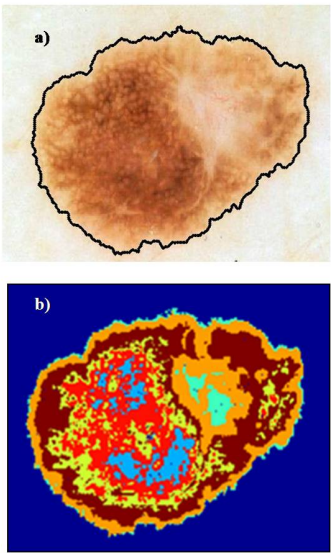

Figure 8. Color segmentation
a) ELM image;
b) lesion map.

correspond to the cluster centroids in 2-D space and consequently will be well-representative of corresponding color regions (or segments) in the starting image. The knowledge of the number of segments is implicit in the peak search, and so is the maximum number *K* of peaks which have to be determined in the 2-D histogram. In our application the algorithm of Koonty [16] has been considered as peaks-picking method. As an example, in Figure 7.c the result of the peaks-picking algorithm is depicted with reference to the 2-D histogram shown in Figure 7.a. when K equal to 14 is selected as maximum number of different color regions.

(iv) Once the peaks are identified, each corresponding hopefully to a segment, the other (non-peaks) histogram bins are attributed to the nearest dominant peak, constituting effectively their domains. Thus, a 2-D histogram is partitioned using its peak bins and an assignment rule (gravity force) which takes into account the strength (height) of the peak and the distance from the pick to the histogram bin under consideration. Figure 7.d shows a partitioned 2-D histogram (after the partitioned 64x64 2-D histogram has been sampled back to its original size by simple replication of the bin labels by 4x4 fold): each color represents a histogram region.

(v) Once the partitioned 2-D is computed, each pixel in the starting image can be directly labeled by taking into account the corresponding values for the two principal components. In particular assigning to each histogram region (or segment) an arbitrary intensity value, a gray-level image (or alternatively a false-color image) can be obtained where different regions are easily identified (see Figure 8).

4.2.2. Texture extraction. As to the search for the occurrence of texture, a combination of two different techniques (*structural* and *spectral methods* [17]) has been designed. As shown in the diagram (Figure 9), the proposed algorithm is arranged into two processing paths, which share the input 8-bit grey-level image extracted from the ELM color image at first stage:

(i) The structural technique, which is intended to search for primitive structures such as lines and/or points which can constitute a texture, can identify local discontinuities by comparing the monochromatic image with its version obtained by a suitable median filter, followed by a close-opening operation, which deletes eventual isolated points. An example of the result of such a processing can be seen in Figure 10, where the small areas appearing between network structures are visible.

(ii) The spectral technique is based on the Fourier analysis of the grey-level image. It is useful to determine the spatial period of the texture, thus allowing the identification of the only regions where a network exists. More in depth, a sequence of Fast Fourier Transform (FFT), high-pass filtering, Inverse Fast Fourier Transform (IFFT) and suitable thresholding has been adopted on the purpose, in order to disregard the local discontinuities which are not clearly associated to a network. The result of this phase is a "regions with network" mask.

Finally two masks are applied to the "local discontinuities" image: the "regions with network" mask, and the mask returned by the image segmentation phase. As a final result, a "network image", where the areas belonging to the lesion and constituting the pigment network are highlighted, is achieved.

4.3. Feature classification

The classification of the morphological and/or chromatic features extracted from the lesions through the algorithms previously described can be viewed as a

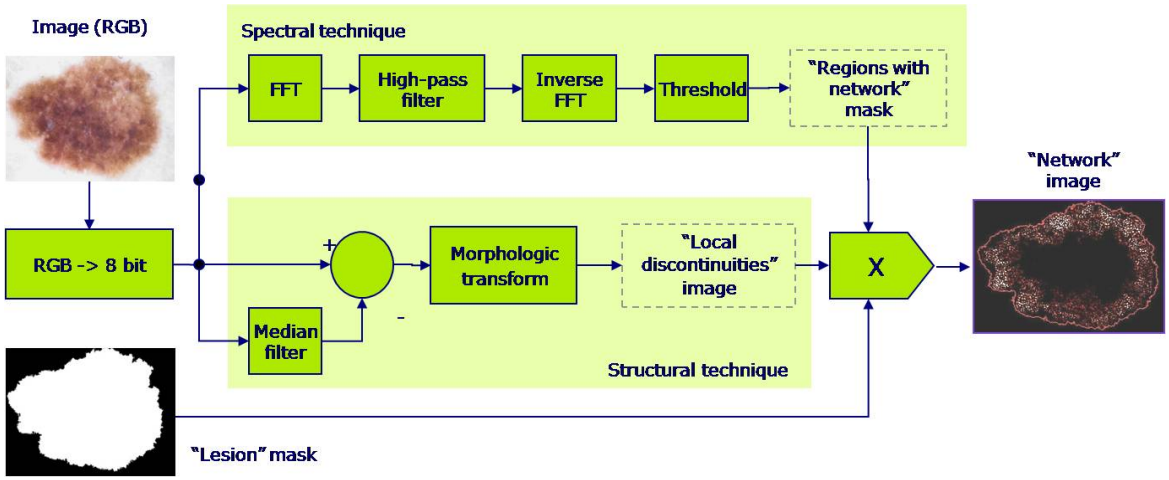

Figure 9. Diagram of Texture extraction

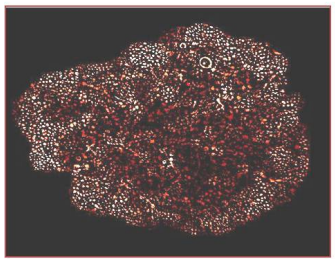

Figure 10. "Local discontinuities" image

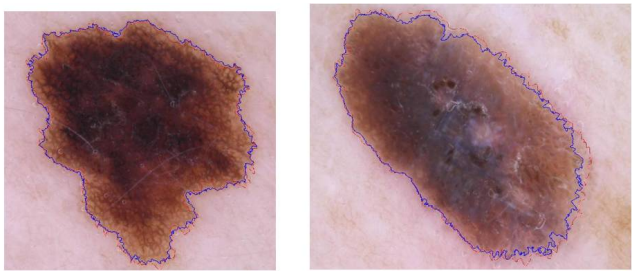

Figure 11. Validation of the Boundary detection stage

problem of data mining.

A well-known class of solutions is represented by *Decision Tree Classifiers*, which belong to the supervised Machine Learning techniques [18].

A Decision Tree Classifier is a predictive model, trained (or induced) by adopting a suitable dataset with respect to which classification results are already available. More in depth, given a collection of objects (each one described by a set of attributes) a Decision Tree is a graph, wherein each internal node stands for an attribute, each arc toward a child node defines a property related to the parent node and finally a terminal node (or leaf) constitutes a classification result (a single value for the attribute adopted as class discriminator). The paths constituted by internal nodes with a parent-child relationship and the corresponding arcs define the rules of the predictive model that can be adopted for classifying new collections of objects.

The Decision Tree Technique can be generally preferred to other solutions (also including Artificial Neural Networks and Support Vector Machines) because Decision Tree Classifiers are often fast to train and apply and generate easy to understand rules. Many induction algorithms have been proposed in literature, which are different for the type (discrete and/or continuous) of attributes they can apply to and the parameter adopted as performance index for the evaluation of the goodness of induction. Probably the *C4.5* algorithm [18] is the most widely adopted for decision tree induction. It can be related to attributes varying into both discrete and continuous range, whereas the *information gain* (relative entropy or Kullback-Leibler divergence) is considered as leading parameter in the splitting procedure (i.e. identification of a significant attribute and its corresponding optimal value to segment the collection into suitable groups). Moreover the C4.5 algorithm tries to prevent the *over-fitting condition* by implementing a *pruning strategy*. Given a large training set, in fact, decision tree classifiers could produce rules that perform well on the training data but do not generalize well to unseen data. In particular the C4.5 is able to identify sub-trees that do not contribute significantly to predictive accuracy and replacing each by a leaf.

Another popular method for classification is instead *linear logistic regression*: it tries to fit a simple (linear) model to the data through a process which generally reveals quite stable, resulting in low variance but potentially high bias. The tree induction exhibits low bias but often high variance because searches a less restricted space of models, allowing it to capture nonlinear patterns in the data, but making it less stable and prone to over-fitting. Consequently a promising way to deal with classification tasks is to use a combination of a tree structure and logistic regression models resulting in a single tree according to the model proposed in [19]. Thus, the Logistic Model Tree (LMT) has been explored as suitable solution for the classification of the feature of interest (the lesion map resulting from the color segmentation and network/objects resulting from the texture extraction).

5. Experimental results

In order to develop and test the automatic procedure for the diagnosis of digital ELM images a suitable database has been selected. In particular about 300 images have been extracted from CD-ROM interactive atlas of dermoscopy [20] (images supplied by 3 different Institutes: University of Naples Federico II, University of Florence and University of Graz in Austria). The database refers both to cutaneous melanomas and (benignant) melanocytic nevi (also including Clark, Spitz, Reed nevi). For each image, the corresponding clinical and histological analysis are available as well as the 7-Point Check List score computed by a group of three expert physicians coming from University "Federico II (Naples). Very promising results have been achieved both for the boundary detection and classification of features.

5.1. Validation of boundary detection

The group of dermatologist has been asked to draw the lesion contour (as reference) for each digital image of the dataset. Excluding a small group (about 20 cases) for which the boundary detection was badly influenced by the massive presence of hair, a satisfactory

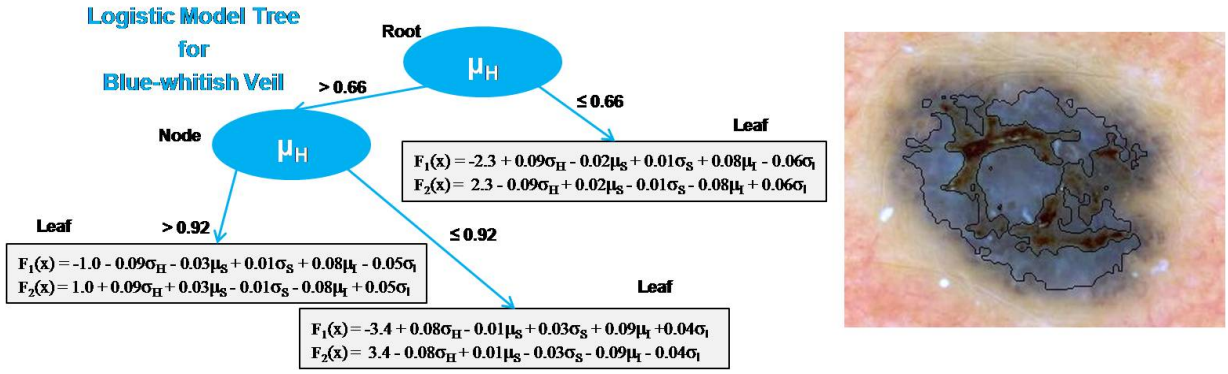

Figure 12. LMT for classification with respect to Blue Veil: Structure of tree and example of detection

agreement with the visual inspection by the group of experts has been accomplished by the automatic procedure (percentage difference for the inner area of the lesion lower than 2%). Three examples of correct boundary extraction are reported in Figure 11 (blue and red contour corresponding respectively to automatic detection and reference).

5.2. Training and Test of Classifiers

For each criterion provided by the 7-Point Check List a classifier has been trained and tested taking into account suitable chromatic and morphological features.

5.2.1. Blue-whitish Veil. The LMT for the detection of Blue-whitish Veil (reported in Figure 12) has been trained on a subset composed of 110 ELM images. The model can be adopted for classify the regions constituting the lesion map resulting from the color segmentation. In particular for each region the components of the corresponding pixels in the *RGB*, *HSI* (Hue, Saturation and Intensity) and CIE *Luv* color spaces [17] has been considered to compute mean value and standard deviation as extracted features (vector $\underline{x}$). In addition the area percentage ($S_{\%}$) of each region with respect to total area of the lesion is taken into account. As you can see in the scheme, three different logistic regression models are computed on the basis of three ranges for the Hue mean value of the region to be analyzed (which can be interpreted as corresponding to blue, red or polychromatic "path"). The regression functions $F_i(\underline{x})$ (with i=1, Blue-Vei region and i=2, no Blue-Veil region) take into account the standard deviation for the Hue component, the mean and standard deviation for Saturation and Intensity components, in order to determine the probability that the color region belongs to an area characterized by the Blue Veil (in Figure 13 the resulting detection of the criterion is depicted).

5.2.2. Regression structures The previous subset of 110 ELM images has been also adopted to train the LMT for the detection of the regression structures throughout the regions resulting from the color segmentation. The vector $\underline{x}$ has been again taken into account as extracted features. As reported in Figure 14, two different logistic models have been computed according to the range wherein the mean value for the Saturation component of the region segment falls. Just five extracted features are truly significant to determine the probability that the color region belongs to an area characterized by Regression (an example of the resulting detection is also reported in Figure 13).

5.2.3. Irregular Pigmentation About this minor criterion, a very simple LMT has been obtained from the training with respect to the segments resulting from

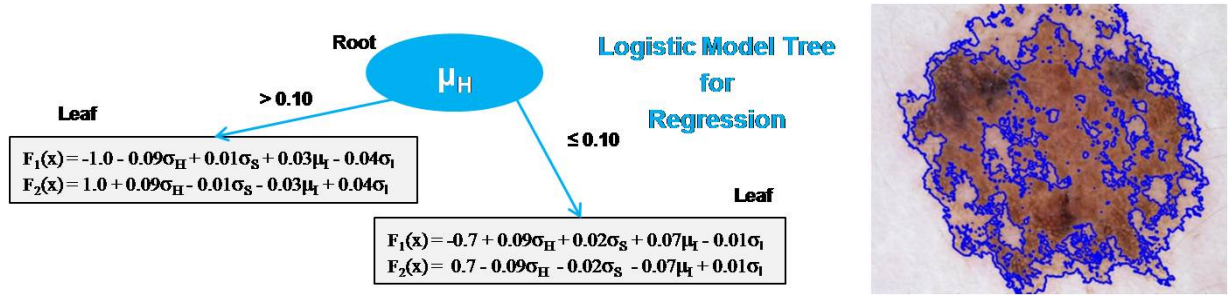

Figure 13. LMT for classification with respect to Regression and example of detection

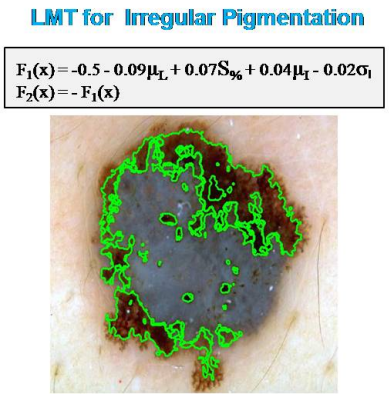

Figure 14. Detection of Irregular Pigmentation

the color segmentation applied to 110 ELM images. The logistic regression model computes the class probabilities taking into account the Intensity and L components (mean and standard deviation), and the area percentage extracted for each color segment of the image (see Figure 14).

5.2.4. Atypical Pigmented Network. The LMT classifier is shown in Figure 15. It can be used to classify the morphological structures resulting from the texture extraction. In particular the following 13 features have been extracted from each network:

- mean value (μ), standard deviation (σ) and their ratio (r), for each *HSI* color component picked at the centers of the objects (local areas) constituting the network;
- mean value (μ_A), standard deviation (σ_A) and their ratio (r_A), for the area of each object of the network expressed as a number of pixels;
- the *area percentage* ($A_{\%}$) of the pigmented network with respect to total area of the lesion.

The LMT trained on a suitable subset of 115 images consider just five measured parameters (μ_H, σ_H , μ_A, σ_A, $A_{\%}$) as truly significant for classifying the network as atypical (an example is depicted in Figure 15).

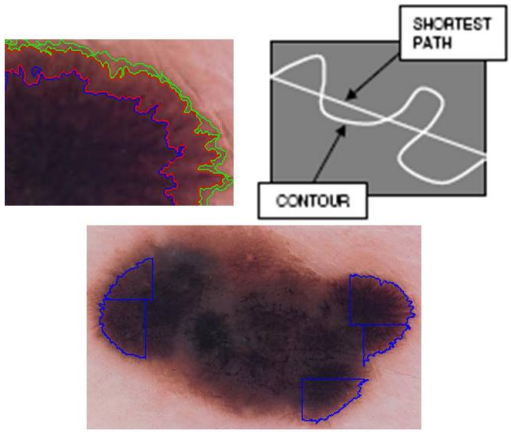

Figure 16. Detection of Irregular Streaks

5.2.5. Irregular Streaks The detection of this minor criterion is based on the local analysis of the lesion contour which is split into 10 equally length segments. Then a color segmentation of the region of interest is performed in order to seek for the black/brown dermoscopic structures (see Figure 16). Finally a morphological irregularity index is computed (as ratio of number of pixels constituting the lesion contour and the shortest path) and compared with a suitable threshold resulting from the statistical analysis carried out.

The detection procedures above described have been verified with respect to a large Test Database constituted by 200 ELM images of skin lesions (including melanomas, Clark, Spitz and Reed nevi).

A brief summary of the validation results about the detection of each criterion is reported in Table II in terms of the achieved *sensitivity* (ratio of corrected classification and total number of images characterized by the criterion of interest) and *specificity* (ratio of corrected classification and total number of images where the considered feature is absent). Both the performance index are ever greater than 0.80 for all five criteria.

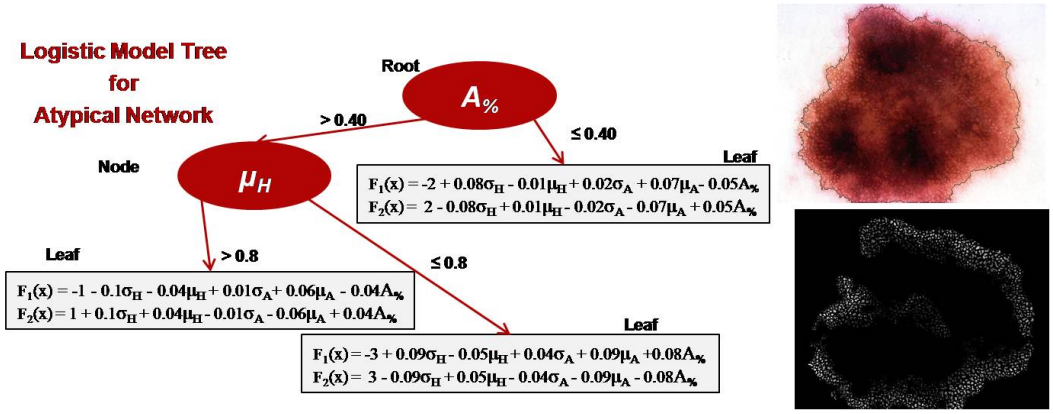

Figure 15. Atypical Pigmented Network: LMT and example of detection

Table 2. the 7-point Check List score system

ELM criterion	Sensibility (%)	Specificity (%)
Major criteria		
Atypical network	80	82
Blue-whitish veil	90	93
Minor criteria		
Irregular streaks	86	88
Irregular pigmentation	87	90
Regression structures	80	83

Taking into account the 7-Point Check List score system, the whole diagnostic software provided a *lesion sensitivity* and *specificity* greater than 0.85 which are in agreement with the results of dermatologist's application known in literature [3].

6. Conclusions

In the paper an automatic measurement system for the diagnosis of melanoma based on 7-points check list applied on epiluminescence microscopy (ELM) skin lesion images is proposed. The achieved performance are very promising and the whole diagnostic system will be used for both screening campaign and follow-up of suspicious lesions. Future work will be focused to *i)* develop suitable algorithms for the detection of the *Atypical Vascular Pattern* and *Irregular Dots/Globules* and *ii)* include into the system software a quantitative estimation for the reliability concerned with single parameter detection and the lesion diagnosis.

10. References

[1] S. E. Umbaugh, R.H. Moss, W.V. Stoecker, G.A. Hance, "Automatic color segmentation algorithms with application to skin tumor feature identification", IEEE Eng Med Biol Vol. 12, 1993, pp.75-82.

[2] M. Binder, M. Schwarz, A. Winkler et al. "Epiluminescence microscopy: a useful tool for the diagnosis of pigmented skin lesion for formally trained dermatologists",Arch Dermatol. Vol. 131, 1995, pp. 286-291.

[3] G. Argenziano, G. Fabbrocini, P. Carli et al., "Epiluminescence microscopy for the diagnosis of doubtful melanocytic skin lesions: comparison of the ABCD rule of dermatoscopy and a new 7-point checklist based on pattern analysis", *Arch Dermatol*. Vol. 134, 1998, pp. 1563-1570.

[4] H. Pehamberger, A. Steiner, K. Wolff, "In vivo epiluminescence microscopy of pigmented skin lesions: Pattern analysis of pigmented skin lesions", J. Am. Acad. Dermatol. Vol. 17, 1987, pp. 571-583.

[5] K. Hoffmann, et alii, "Diagnostic and neural analysis of skin cancer (DANAOS). A multicentre study for collection and computer-aided analysis of data from pigmented skin lesions using digital dermoscopy", Br. J. Dermatol. Vol. 149, 2003, pp. 801-9.

[6] M. Burroni, R. Corona, G. Dell'Eva et al., "Melanoma computer-aided diagnosis: reliability and feasibility study", Clin. Cancer Res. Vol. 10, 2004, pp. 1881-6.

[7] H. Ganster, a. Pinz, R. Röhrer et al., "Automated melanoma recognition", IEEE Trans. Med. Imaging vol. 20, 2001, pp. 233-239.

[8] P. Schmid, "Segmentation of digitized dermatoscopic images by two-dimensional color clustering", IEEE Trans. Med. Imaging Vol. 18, 1999, pp. 164-171.

[9] P. Schmid, J. Guillodb, "Towards a computer-aided diagnosis system for pigmented skin lesions", Comput Med Imaging Graph. Vol. 27 2003, pp. 65–78.

[10] C. Grana, G. Pellacani, R. Cucchiara, S. Seidenari, "A new algorithm for border description of polarized light surface microscopic images of pigmented skin lesions" IEEE Trans. Med. Imaging. Vol. 22, 2003, pp. 959-64.

[11] C. Liguori, A. Paolillo, A. Pietrosanto. "An automatic measurement system for the evaluation of carotid intima-media thickness", IEEE Trans. on Instr. and Meas. Vol. 50, 2001, pp. 1684–1691.

[12] G. Di Leo, G. Fabbrocini, C. Liguori, A. Pietrosanto, M. Scalvenzi, "ELM image processing for melanocytic skin lesion based on 7-point checklist: a preliminary discussion", 13th IMEKO TC-4 Symposium, Vol.2, 2004, pp. 474-479

[13] G. Betta, G. Di Leo, G. Fabbrocini, A. Paolillo, M. Scalvenzi, "Automated Application of the 7-point checklist Diagnosis Method for Skin Lesions: Estimation of Chromatic and Shape Parameters", Instrumentation and Measurement Technology Conference (IMTC) 2005, pp. 1818-1822.

[14] N. Otsu, "A threshold selection method from gray-level histogram", IEEE Transactions on System Man Cybernetics, Vol. SMC-9, N° 1, 1979, pp. 62-66.

[15] A. Levy, M. Lindenbaum, "Sequential Karhuen-Loeve basis extraction and its Application to images", IEEE Trans. on Image Processing Vol. 9, 2000, pp. 1371-1374.

[16] W. Koonty, P.M. Narenda, F. Fukunya, A graph theoretic approach to non-parametric cluster analysis, IEEE Transactions on Computer 25 (1976) 936-944.

[17] R.C. Gonzalez, R.E. Woods, "Digital Image Processing Prentice Hall, New Jersey, 2002.

[18] H. Witten, E. Frank, "Data Mining: Practical Machine Learning Tools and Techniques", Morgan Kaufmann, San Francisco, 2005.

[19] N. Landwehr, M. Hall, E. Frank, "Logistic Model Trees",14th Europ. Conference on Machine Learning, 2003.

[20] G. Argenziano, H.P. Soyer, V. De Giorgi et al., "Interactive Atlas of Dermoscopy", EDRA Medical Publishing & New Media, Milan, Italy, 2002.